Geometry of the Fluorides, Oxofluorides, Hydrides, and Methanides of Vanadium(V), Chromium(VI), and Molybdenum(VI): Understanding the Geometry of Non-VSEPR Molecules in Terms of Core Distortion

Ronald J. Gillespie,* Ian Bytheway, Ting-Hua Tang, and Richard F. W. Bader

Department of Chemistry, McMaster University, Hamilton, Ontario L8S 4M1, Canada

Received November 2, 1995[⊗]

This paper describes a study of the topology of the electron density and its Laplacian for the molecules VF_5, VMe_5, VH_5, CrF_6, $CrMe_6$, $CrOF_4$, $MoOF_4$, CrO_2F_2, $CrO_2F_4^{2-}$ and $CrOF_5^-$ all of which, except VF_5, CrF_6, and $CrOF_5^-$ have a non-VSEPR geometry. It is shown that in each case the interaction of the ligands with the metal atom core causes it to distort to a nonspherical shape. In particular, the Laplacian of the electron density reveals the formation of local concentrations of electron density in the outer shell of the core, which have a definite geometrical arrangement such as four in a tetrahedral arrangement or five in a square pyramidal or trigonal bipyramidal and six in an octahedral arrangement. Ligands that are predominately covalently bonded are found opposite regions of charge depletion between these core charge concentrations. In VH_5, VMe_5, $CrOF_4$, and $MoOF_4$, these core charge concentrations have a square pyramidal arrangement, and the regions of charge depletions have the corresponding inverse square pyramidal arrangement so that these molecules have a square pyramidal geometry rather than a trigonal prism geometry. In $CrMe_6$, there are five core charge concentrations with a trigonal bipyramidal arrangement so that the regions of charge depletion have a trigonal prismatic arrangement and the molecule has the corresponding trigonal prism geometry rather than an octahedral geometry. In contrast, molecules in which the only ligand is the more ionically bound fluorine are less affected by core distortion and have VSEPR-predicted structures. The unexpected bond angles in CrO_2F_2 and the preference of $CrO_2F_4^{2-}$ for a *cis* structure are also discussed in terms of the pattern of core charge concentrations.

Introduction

In two previous papers[1,2] we have shown how the Laplacian of the electron density can be used to provide an increased understanding of the structures of molecules that do not appear to conform to the VSEPR model.[3,4] In this paper we use the same method to examine the geometries of some of the fluorides, oxofluorides, hydrides, and methanides of V(V), Cr(VI), and Mo(VI), some of which also do not conform to the VSEPR model. X-ray and electron diffraction studies have shown that whereas MoF_6, WF_6 , WCl_6, WBr_6, TiF_6^{2-}, $ZrCl_6^{2-}$, $Mo(NMe_2)_6$, $W(NMe_2)_6$ and $W(OMe)_6$ all have the VSEPR predicted octahedral geometry,[5] WMe_6 and $ZrMe_6^{2-}$ have a trigonal prismatic geometry.[6,7] Similarly, whereas VF_5, $NbCl_5$, $TaCl_5$, and $TaBr_5$, have all been found to have the VSEPR predicted trigonal bipyramidal geometry with longer axial than equatorial bonds,[8] $TaMe_5$ has a square pyramidal geometry.[9] The d^0 transition metal oxohalides $CrOF_4$, $MoOF_4$, and WOF_4 have a non-VSEPR square pyramidal geometry[3,9] whereas SOF_4 has the expected trigonal bipyramidal geometry.[1] Although CrO_2F_2 and CrO_2Cl_2 have tetrahedral structures[3,10] like SO_2F_2 and SO_2Cl_2 , they are exceptions to the predictions of the VSEPR model, according to which double bond domains are larger than single bond domains, because the O═M═O angles are smaller than the tetrahedral angle, rather than larger, and the Hal−M−Hal angles are larger, rather than smaller than the tetrahedral angle. The related octahedral anion $CrO_2F_4^{2-}$ is also an exception to the VSEPR model in that the two double-bonded oxygen ligands occupy *cis* rather than *trans* positions.[11]

A basic assumption of the VSEPR model is that the core of the central atom in an AX_n molecule is spherical and has no influence on the geometry of the molecule. Although this assumption is valid for nonmetal molecules it appears that it is generally not valid when this atom is a metal. For example, we have shown recently[2] by an examination of the Laplacian of the electron density of the metal atom that in the heavier group II dihalide molecules the core of the metal atom is distorted to a nonspherical shape by the formation of four tetrahedrally arranged local charge concentrations. This distortion causes these molecules to have an angular geometry rather than the linear geometry predicted by both the VSEPR model and the ionic model.

In discussing the topology of the Laplacian of the electron density, $\nabla^2\rho$, in terms of its critical points it is convenient to define the function $L = -\nabla^2\rho$. The local maxima or (3, −3) critical points in L denote regions of local charge concentration, that is regions in which there is a partial condensation of the electrons into pairs such that this region is dominated by the presence of a single pair of electrons.[12] The local maxima (charge concentrations) in the valence shell of a nonmetal or

[⊗] Abstract published in *Advance ACS Abstracts,* June 1, 1996.

(1) Gillespie, R. J.; Bytheway I.; DeWitte, R. S.; Bader, R. F. W. *Inorg. Chem.* **1994**, *33*, 2115.
(2) Gillespie, R. J.; Bytheway I.; Gillespie, R. J.; Tang, T.-H.; Bader, R. F. W. *Inorg. Chem.* **1995**, *34*, 2407.
(3) Gillespie, R. J.; Hargittai, I. *The VSEPR Model of Molecular Geometry;* Allyn and Bacon: Boston, MA, 1991.
(4) Gillespie, R. J. *Chem. Soc. Rev.* **1992**, 59. Gillespie, R. J., Robinson, E. A. *Angew. Chem., Int. Ed. Engl.* **1996**, *35*, 495.
(5) For references to individual structures, see ref 18.
(6) Haaland, A.; Hammel. A.; Rypdall, K.; Volden, H. V.: *J. Am. Chem. Soc*. **1990,** *112*, 4547.
(7) Morse, P. M.; Girolami, G. S. *J. Am. Chem. Soc*. **1989**, *111*, 4114.
(8) Haaland, A.; Hammel, A,; Rypdal, K.; Verne, H. P.; Volden, H. V.; Pulham, C.; Brunvoll, J.; Weidlein, J.; Greune, M. *Angew. Chem.* **1992,** *104*, 1532.
(9) Christe, K. O.; Wilson, W. W.: Bougon, R. A. *Inorg. Chem*. **1986,** *25*, 1904.
(10) French, R. J.; Hedberg, L; Hedberg, K.;, Johnson, B. M. *Inorg. Chem.* **1983**, *22*, 892.
(11) Brown, S. D.; Green, P. J. Gard G. L. *J. Fluorine Chem*. **1975,** *5*, 203.

S0020-1669(95)01420-0 CCC: $12.00

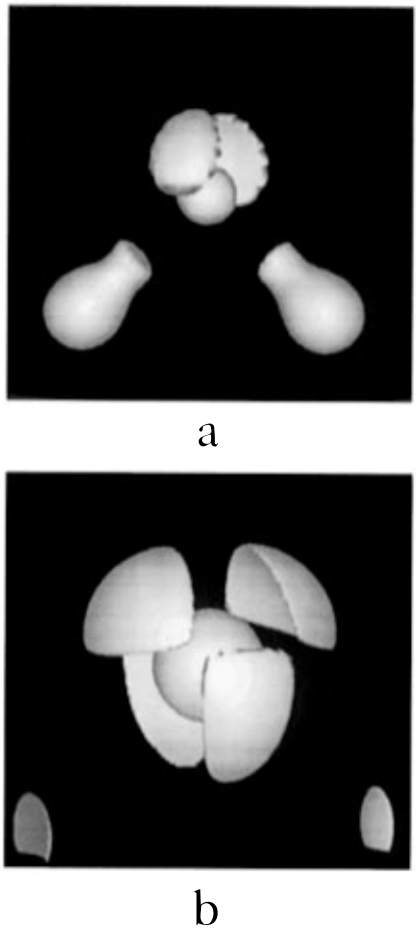

Figure 1. Envelopes of the Laplacian of the electron density $\rho(r)$ for H_2S (a) and BaH_2 (b). These envelopes define regions wherein electronic charge is locally concentrated, $L > 0$. The four envelopes in the valence shell of S have an approximately tetrahedral arrangement and define two nobonded charge concentrations (CC's) and two bonding CC's, the envelopes of the latter being contiguous with the regions of charge concentration on the protons. The four envelopes in b are in the outer shell of the core of Ba and define four CC's with an approximately tetrahedral arrangement of which two are ligand opposed. The two lower partial envelopes are associated with the protons.

the outer shell of the core of a metal define the vertices, *V*, of a polyhedron called an atomic graph. The unique pair of trajectories of the gradient of *L* that originate at a (3, −1) critical point or saddle point between two maxima and terminate at neighboring vertices define the edges *E* of the polyhedron and the set of trajectories that arise at a (3, +1) critical point define the faces *F*. The face critical points are where *L* attains a local minimum value, that is where there is a maximum local depletion of electron density. The numbers of each type of critical point satisfy the Euler polyhedral formula $V - E + F = 2$.

The typical pattern of electron localization revealed by the topology of the Laplacian distribution in a nonmetal molecule exhibits bonding and nonbonding charge concentrations in the valence shell of the nonmetal atom as is illustrated in Figure 1a for the sulfur atom in H_2S. There are four approximately tetrahedrally disposed charge concentrations (CC's) as anticipated by the VSEPR model—two bonding CC's and two nonbonding (lone pair) CC's surrounding an almost perfectly spherical core. The bonding CC's result from the *attraction* of the ligands for the valence shell electrons and the nonbonding CC's from the operation of the Pauli principle.

In contrast, the pattern of electron localization in a molecule of a metal differs in two important ways from that for a nonmetal molecule, as is illustrated by the Laplacian of the electron density for the barium atom in BaH_2 (Figure 1b).[2] In this molecule, as in all other molecules of the metals from period 4 and beyond that we have studied, there is no valence shell charge concentration but there are charge concentrations in the outer shell of the core, which is therefore not spherical, unlike the core of a nonmetal atom. The shell structure of an atom is clearly visible in *L*,[12] and as shown previously,[2] the shell in which the charge concentrations occur in BaH_2 is the 5th shell, that is the outer shell of the core.

In BaH_2 there are four such charge concentrations (Figure 1b). Two of them are in positions on the opposite side of the core from the ligands and the other two complete an approximately tetrahedral arrangement. They arise from the combined effect of the Pauli principle and the *repulsion* between the ligands and the core electrons.[2] In contrast the four charge concentrations in the valence shell of a nonmetal atom such as sulfur in H_2S result from the combined effect of the Pauli principle and the *attraction* of the ligand atom cores for the valence electrons of sulfur (Figure 1a). In response to this pattern of localization of the core electrons in barium, which is also found in the difluoro and dimethyl molecules, the ligands tend to occupy two of the four faces of the tetrahedral arrangement of CC's. These are the positions of face or (3, +1) critical points in *L* where *L* has a minimum value, that is where there is a local depletion of charge. The bonding electron pairs of the ligands are attracted toward these regions of charge depletion and repelled away from the (3, −3) maxima or regions of charge concentration in the outer shell of the core. Repulsion between the ligands, however, tends to give the linear VSEPR geometry so that the bond angles of the group 2 dihalides decrease toward the tetrahedral angle with increasing size and polarizability of the core from Ca to Ba. The increasing polarizability of the core results in an increasing distortion of the core, and the increasing size of the core results in a reduced repulsion between the ligands, which together lead to a smaller bond angle.

In this paper we show that the cores of V(V), Cr(VI), and Mo(VI) fluorides, oxofluorides, hydrides, and methanides, are similarly distorted by the formation of core charge concentrations and we discuss how these core CC's affect the geometry of these molecules. We have studied the molecules VF_5,VMe_5, VH_5, CrF_6, $CrMe_6$, $CrOF_4$, $MoOF_4$, CrO_2F_2, $CrO_2F_4^{2-}$, and $CrOF_5^-$ all of which, except VF_5, CrF_6, and $CrOF_5^-$ have non-VSEPR structures.

Calculations

The molecular energies and electron densities were determined in single determinant SCF calculations using Gaussian 92.[13] The 6-311++G(2d,2p) basis set was used for oxygen, sulfur carbon, fluorine, and hydrogen,[13] a (14s, 11p, 6d//10s, 8p, 3d) set for chromium and vanadium,[14] and a (15s 9p 6d//5s 3p 2d) basis set for molybdenum.[15]

While post Hartree−Fock calculations are required to definitively establish the geometries associated with the global energy minimum in certain of these systems, the topological properties of the electron

(12) Bader, R. F. W. *Atoms in Molecules: A Quantum Theory;* Oxford University Press: Oxford, England, 1990. Bader, R. F. W.; Gillespie, R. J. ; MacDougall, P. J. *J. Am. Chem. Soc.*, **1988**, *110*, 7329.

(13) Frisch, M. J.; Trucks, G. W.; Head-Gordon, M.; Gill, P. M. W.; Wong, M. W.; Foresman, J. B.; Johnson, B. G.; Schlegel, H. B.; Robb, M. A.; Replogle, E. S.; Gomperts, R.; Andres, J. L.; Raghavachari, K.; Binkley, J. S.; Gonzalez, C., Martin, R. L.; Fox, D. J.; DeFrees, D. J.; Baker, J.; Stewart, J. J. P.; Pople, J. A. *Gaussian 92*, Gaussian, Inc., Pittsburgh, PA, 1992.

(14) Wachters, A. J. H. *J. Chem. Phys.* **1978,** *52*, 1033. As described in GAMESS. Schmidt, M. W.; Baldridge, K. K.; Boatz, J. A.; Jensen, J. H.; Koseki, S.; Gordon, M. S.; Nguyen, K. A.; Windus, T. L.; Elbert, S. T. *QCPE Bull.* **1990**, *10*, 52.

(15) Sakai, Y.; Tatewaki, H.; Huzinaga, S. *J. Comput. Chem.* **1982,** *3*, 6.

Table 1. Calculated Energies and Geometries[a]

molecule	geometry[b]	relative energy (kcal mol^{-1})	bond length (Å)	bond angle (deg)
VF_5	tbp	0.0	1.7250 (ax)	90.0
			1.6818 (eq)	120.0
VF_5	sp	2.4	1.6615 (ax)	105.2 ($F_{ba}-M-F_{ax}$)
			1.7099 (ba)	86.1 (Fb_a-M-F_{ba})
VH_5	tbp	26.8	1.7214 (ax)	90.0
			1.6049 (eq)	120.0
VH_5	sp	0.0	1.6461 (ax)	120.7 ($F_{ba}-M-F_{ax}$)
			1.5953 (ba)	74.9 ($F_{ba}-M-F_{ba}$)
$V(CH_3)_5$	sp		2.0161 (ax)	112.2 ($F_{ba}-M-F_{ax}$)
			2.0802 (ba)	81.8 ($F_{ba}-M-F_{ba}$)
CrF_6	oct	0.0	1.6790	90.0
CrF_6	tp	6.9	1.6967	83.9; 96.1[c]
$Cr(CH_3)_6$	tp		2.1514	89.5 (C−Cr−C)[c]
				71.3 (C−Cr−C)[c]
$CrOF_4$	tbp	11.5	1.7151 (ax)	98.5 ($O-Cr-F_{ax}$)[d]
			1.6839 (eq)	123.0 ($O-Cr-F_{eq}$)[d]
			1.4702 (O)	
$CrOF_4$	sp	0.0	1.4609 (O)	105.3 (O−Cr−F)
			1.6997 (F)	86.0 (F−Cr−F)
$MoOF_4$	tbp	11.1	1.8060 (F_{ax})	98.5 ($O-Mo-F_{ax}$)[d]
			1.7873 (F_{eq})	123.0 ($O-Mo-F_{eq}$)[d]
			1.5920 (O)	
$MoOF_4$	sp	0.0	1.5871 (O)	104.1 (O−Mo−F)
			1.7972 (F)	86.6 (F−Mo−F)
CrO_2F_2	tet	0.0	1.4984 (O)	108.8 (O−Cr−O)
			1.6928 (F)	108.2 (F−Cr−F)
$CrOF_5^-$	oct		1.4913 (O)	94.7 ($O-Cr-F_{eq}$)
			1.7530 (F_{eq})	
			1.8318 (F_{ax})	
cis-$CrO_2F_4^{2-}$	oct	0.0	1.5471 (O)	101.1 (O−Cr−O)
			1.9467 (F_{eq})	169.1 ($O-Cr-F_{eq}$)
			1.8736 (F_{ax})	89.1 ($O-Cr-F_{ax}$)
trans-$CrO_2F_4^{2-}$ oct	oct	42.2	1.6052 (O)	180.0 (O−Cr−O)
			1.8596 (F)	90.0 (F−Cr−F)

[a] Basis sets are described in the text. VH_5 molecules were calculated at MP2(full), with all others at the single determinant SCF level. [b] Key: tbp = trigonal bipyramid; sp = square pyramid; oct = octahedron; tp = trigonal prism; tet = tetrhedron. [c] First value is for the angle between bonds to atoms in triangular face. Second value is for bonds to corresponding atoms in opposite triangular faces. [d] These angles were held fixed in an otherwise free optimization, as this is not a minimum energy geometry.

density and its Laplacian are well established at the Hartree−Fock level.[16] Our calculations predict the correct energy ordering of the geometries and the calculated differences in energy are in satisfactory agreement with the more detailed calculations (Table 1).

Results and Discussion

Topology of the Electron Density and the Nature of the Metal−Ligand Bond. Table 1 gives the calculated and experimental bond lengths and angles for each of the molecules studied and their relative energies. The topology of the electron density for each of the molecules yields the anticipated structures in which each ligand is linked to the metal atom by a bond path as illustrated for VF_5, $V(CH_3)_5$, and $CrOF_4$ in Figure 2, which also shows the zero flux surfaces that separate the molecules into their component atoms.[12] Table 2 gives the electron density ρ_b, $L_b = (-\nabla^2\rho)_b$, and the energy density H_b[17] at the critical point of each bond path, the distance of the critical point from the nucleus of the metal atom, r_b, and the charge on each atom, q(X).

In the "ionic" limit these molecules are described as consisting of V^{5+} and Cr^{6+} (or Mo^{6+}) cores surrounded by the appropriate number of anionic ligands. However, the charges on the metal atoms are considerably smaller than this ionic description implies, ranging from a maximum of +3.3 in the fluorides to +2.7 in the oxofluorides and from +2.0 to +1.5 in the methanides and hydrides. The charges on the ligands are typically −0.6 for F, −0.5 to −0.8 for O and −0.3 for H and CH_3. These charges are smaller than those observed for group 1 and 2 metal fluorides, hydrides, and methanides and, somewhat surprisingly, smaller than those for the corresponding nonmetal fluorides and oxofluorides such as SOF_4 in which the charge on sulfur is +4.2.[1] These charges indicate that there is a considerable sharing of electrons between the ligands and the metal; in other words, there is an appreciable covalent character to the bonds, which increases in the series F, O, (H, CH_3). This conclusion is supported by the values of ρ_b and H_b listed in Table 2.

For all the bonds the relatively large values of ρ_b and the negative values of H_b are well removed from the limiting values characteristic of ionic closed-shell interactions for which $\rho_b < 0.07$ and H_b is greater than zero or has a very small negative value. For the bonds to oxygen the large values of ρ_b coupled with large negative values for H_b are indicative of a strong shared interaction, while the large positive values of $\nabla^2\rho$ indicate a polar displacement toward oxygen consistent with the view that the MO bonds are strong polar double bonds. Neuhaus *et al.*[18] find values of ρ_b and H_b for the M−N and M−O bonds in oxo and nitrido fluorides of Mo, W, Re, and Os that are very similar to the values for the Cr−O and Mo−O bonds listed in Table 2, indicating that in these molecules also the M−N and M−O bonds are strong covalent multiple bonds. That the Cr−O and Mo−O bonds are strong covalent bonds is supported by the very short bond lengths of 1.46−1.50 and 1.59 Å compared

(16) Gatti, C.; MacDougall, P. J.; Bader, R. F. W. *J. Chem. Phys.* **1988**, *88*, 3792.
(17) Cremer, D.; Kraka, E. *Angew. Chem.* **1984**, *96*, 612; *Angew. Chem., Int. Ed. Engl.* **1984**, *109*, 5917.
(18) Neuhaus, A.; Veldkamp, A.; Frenking, G. *Inorg. Chem.* **1994**, *33*, 5278.

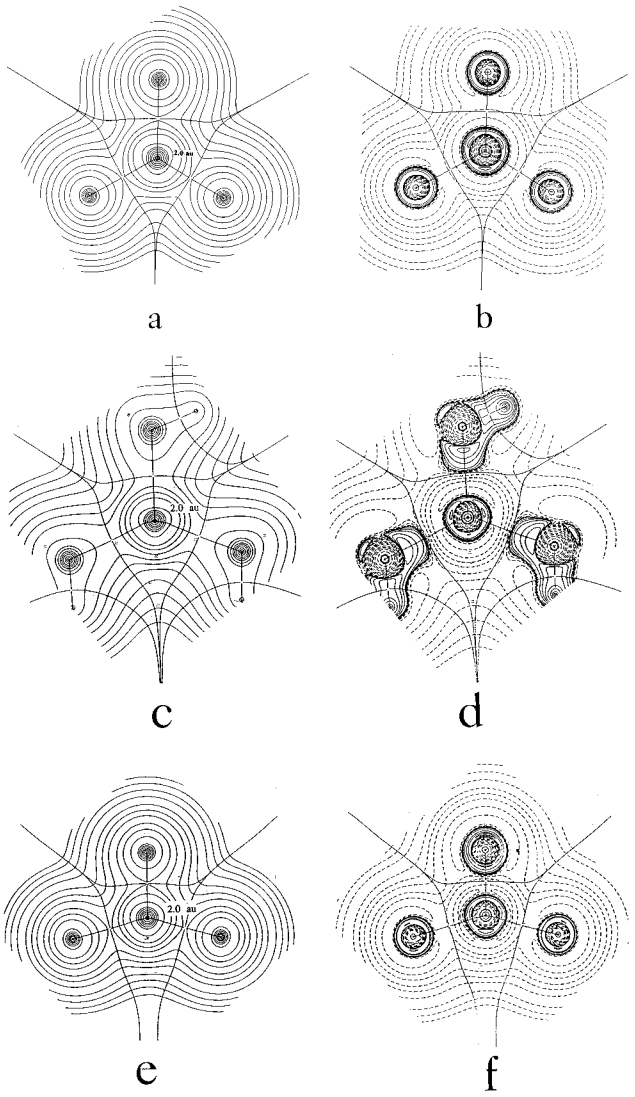

Figure 2. Contour maps of $\rho(r)$ and $L = -\nabla^2\rho(r)$ for the equatorial plane of trigonal bipyramidal geometry of VF_5 (a and b), and for a plane through the axial and two basal ligands in the square pyramidal geometries of VMe_5 (c and d), and $CrOF_4$ (e and f). The contours are in atomic units. The outer contour in ρ is 0.001 and the other contours increase in value in the order 2×10^n, 4×10^n, 8×10^n with n beginning at -3 and increasing in steps of 1. This geometric progression also defined the contour values of L, positive values being denoted by solid lines and negative values by dashed lines. Note that the $\rho = 2.0$ contour line of the Cr and V cores are distinctly polarized, reflecting the presence of the core CC's found in the contour maps of L.

with the sum of the single bond covalent radii of 1.76 and 1.88 Å, respectively, indicating considerable multiple bond character.[10,19]

For the MF bonds the values of ρ_b and H_b indicate that there is less shared density than in the MO bonds, confirming the conclusion from the atomic charges that these bonds are more ionic than the MO bonds. It is interesting to note that, consistent with VSEPR predictions, these values also indicate that MF(ax) bonds are more ionic and weaker than MF(eq) bonds in trigonal bipyramidal molecules.

The M−C and M−H bonds exhibit the smallest values of ρ_b, while being the least polar and having very small values for $\nabla^2\rho$, the latter being indicative of a balance between the contraction of the density perpendicular and parallel to the bond path.[12] These are properties not previously found for bonds to carbon or hydrogen and when contrasted with the values for typical CH bonds (Table 1), indicate a weak shared interaction. The lengths of the V−C, V−H, and Cr−C bonds also indicate that these bonds are rather weak as in each case they are considerably longer than calculated from single bond radii. V−C = 2.05 Å (average) compared to 1.93 Å, Cr−C = 2.15 Å compared to 1.91Å, and V−H = 1.62 Å(average) compared to 1.48 Å.[19]

It is clear from the contour maps for the total density of $CrOF_4$ and $V(CH_3)_5$ in Figure 2 that the electron density of the carbon atom of a methyl group is more equally shared with the metal atom than is the density in the M−O and M−F bonds, the electron density of a fluorine or oxygen atom being more localized in the individual atomic basins. However, the oxygen density is more polarized toward the metal as can be seen from the shape and magnitude of the contours meeting at the bond critical point of the M−O bond which have twice the value of the corresponding contours for the M−F bond.

In the contour maps of L (Figure 2) there is a bonded charge concentration in the valence shell of oxygen in these molecules and a large, spatially more pronounced one on the carbon atom of a methyl ligand. Neuhaus *et al.*,[18] commenting on the pronounced covalent nature of the nitrido and oxo bonds to Mo, W, Re, and Os, noted the similar presence of bonded charge concentrations on the N and O atoms. In VH_5 the corresponding bonded CC envelops the proton and is strongly polarized toward the metal atom, being similar in form and size to that on carbon. As can be seen in the relief map of L for $CrOF_5^-$ in Figure 3 the fluorine ligands, in contrast, expose a (3, +1) critical point toward the metal atom, a feature that is characteristic of polar bonds to fluorine.

In all the transition metal molecules discussed in this paper we have found charge concentrations in the metal core similar to those found in the group 2 dihalides. In most cases these charge concentrations are ligand opposed and in all cases they form a polyhedron with (3, −1) critical points in the edges and (3, +1) critical points in the faces. These (3, +1) critical points define the regions of local charge depletion.[12] As in the case of the group 2 dihalides, the geometry of a molecule is determined by the tendency of some ligands to occupy sites facing these regions of local charge depletion giving a geometry that is not always the VSEPR predicted geometry. In the molecules that we discuss in this paper the ligands −H, $-CH_3$, and =O are always found in these sites and all these molecules have non-VSEPR geometries. In contrast when the ligand is F (and probably Cl, Br, and OR) the molecules have the VSEPR predicted geometry. We have seen that −H, $-CH_3$, and =O are more covalently bonded than −F, and as can be seen from the plots of ρ and of L in Figure 2, they distort the core more than the more ionically bound F. It appears that the interaction of F with the core in the vanadium and chromium fluorides is sufficiently weak that the ligand−ligand and bond−bond repulsions dominate and give the VSEPR geometry. In contrast the core of a group 2 metal is more polarizable and therefore more easily distorted to form charge concentrations than the cores of V(V), Cr(VI) and Mo(VI) so that even F, which in these molecules exhibits a small bonding CC, interacts sufficiently with the core to occupy positions facing (3, +1) critical points giving a non-VSEPR geometry. We now discuss each of the molecules in detail.

Vanadium Pentafluoride, Pentamethanide, and Pentahydride. An extensive study of the calculated structures of VF_5, VH_5, $TaCl_5$, TaH_5, and $TaMe_5$ at various levels of theory has

(19) Covalent radii for O and F (O = 0.62 Å and F = 0.54 Å) were taken from: Gillespie, R. J.; Robinson, E. A. *Inorg. Chem.* **1992**, *31*, 1960 and unpublished work. These values are smaller than those that are frequently given for these radii but comparison with bond lengths calculated from the more commonly used larger values would only indicate a still greater multiple bond character. The other radii used were commonly accepted values, see, for example: Huheey, J. E.; Keiter, E. A.; Keiter, R. L. *Inorganic Chemistry*; Harper Collins: New York, 1993.

Table 2. Properties of the Electron Density Distributions[a]

molecule	bond	ρ_b	H_b	$\nabla^2\rho_b$	r_b(M)	q(M)	q(ligand)
VF_5(tbp)	$V-F_{ax}$	0.170	−0.054	+0.993	1.647	+3.124	−0.659
	$V-F_{eq}$	0.192	−0.075	+0.989	1.601		−0.609
VF_5(sp)	$V-F_{ax}$	0.202	−0.084	+1.061	1.581	+3.127	−0.602
	$V-F_{ba}$	0.178	−0.061	+0.971	1.629		−0.631
VH_5(tbp)	$V-H_{ax}$	0.101	−0.038	+0.042	2.017	+1.839	−0.529
	$V-H_{eq}$	0.129	−0.061	+0.043	1.961		−0.260
VH_5(sp)	$V-H_{ax}$	0.115	−0.048	+0.039	1.932	+1.691	−0.454
	$V-H_{ba}$	0.130	−0.061	−0.013	1.939		−0.309
VMe_5(sp)	$V-C_{ax}$	0.130	−0.059	+0.049	1.882	+2.078	−0.489
	$V-C_{ba}$	0.117	−0.048	+0.025	1.987		−0.397
	$C_{ax}-H$	0.281	−0.325	−1.096	1.271	0.383	−0.035
	$C_{ba}-H$	0.284	−0.330	−1.128	1.275	−0.236	−0.054
CrF_6(oct)	Cr−F	0.204	−0.101	+0.962	1.605	+3.254	−0.542
CrF_6(tp)	Cr−F	0.200	−0.099	+0.762	1.617	+3.089	−0.515
$CrMe_6$(tp)	Cr−C	0.092	−0.043	+0.019	2.017	+1.510	−0.252
	C−H	0.290	−0.341	−1.178	1.277	−0.126	−0.042
$CrOF_4$(tbp)	$Cr-F_{ax}$	0.181	−0.078	+0.881	1.627	+2.926	−0.624
	$Cr-F_{eq}$	0.198	−0.092	+0.909	1.597		−0.574
	$Cr-O_{eq}$	0.387	−0.358	+1.132	1.464		−0.531
$CrOF_4$(sp)	$Cr-O_{ax}$	0.395	−0.371	+1.164	1.458	+2.928	−0.495
	$Cr-F_{ba}$	0.189	−0.084	+0.900	1.163		−0.608
$MoOF_4$(tbp)	$Mo-F_{ax}$	0.170	−0.056	+0.995	1.801	+3.501	−0.648
	$Mo-F_{eq}$	0.179	−0.064	+0.996	1.777		−0.661
	$Mo-O_{eq}$	0.340	−0.297	+1.010	1.608		−0.810
$MoOF_4$(sp)	$Mo-O_{ax}$	0.344	−0.303	+1.003	1.603	+3.499	−0.766
	$Mo-F_{ba}$	0.174	−0.056	+1.104	1.791		−0.683
CrO_2F_2(tet)	Cr−O	0.395	−0.315	+1.164	1.458	+2.689	−0.689
	Cr−F	0.184	−0.074	+1.022	1.599		−0.656
$CrOF_5^-$(oct)	Cr−O	0.355	−0.302	+1.587	1.456	+4.037	−0.578
	$Cr-F_{ax}$	0.129	−0.037	+0.691	1.735		−0.752
	$Cr-F_{eq}$	0.162	−0.059	+0.772	1.656		−0.677
$CrO_2F_4^{2-}$(cis)	Cr−O	0.302	−0.230	+1.098	1.512	+4.683	−0.735
	$Cr-F_{ax}$	0.110	−0.029	+0.524	1.760		−0.778
	$Cr-F_{eq}$	0.091	−0.024	+0.429	1.842		−0.828
$CrO_2F_4^{2-}$(trans)	Cr−O	0.253	−0.160	+1.291	1.551	+4.741	−0.817
	Cr−F	0.113	+0.531	+0.531	1.746		−0.777

[a] ρ_b is the electron density at the bond critical point; H_b is the energy density at the bond critical point; $\nabla^2\rho_b$ is the value of $\nabla^2\rho(-L)$ at the critical point: r_b is the distance of the bond critical point from the nucleus of the metal atom; q(M) is the charge on the metal atom; q(ligand) is the charge on the ligand. All values are in atomic units: 1 au $\rho = e/a_0^3 = 6.478$ e/Å^3; 1 au $H = e^2/a_0^4 = 0.1482$ hartree/Å^3; 1 au $\nabla^2\rho = e/a_0^5 = 24.099$ e/Å^5; 1 au length $= a_0 = 0.5292$ Å.

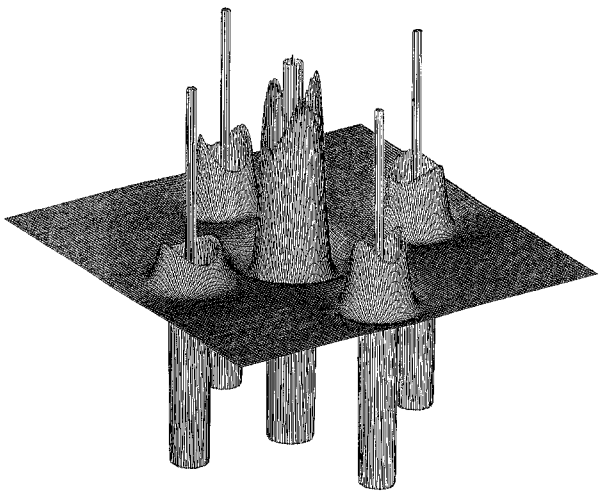

Figure 3. Relief of L for the octahedral molecule $CrOF_5^-$ in the plane through the axial O nucleus and three F nuclei. The ligand opposed charge concentrations are found in the outer shell of the core of Cr, the third quantum shell. Note that the valence shell charge concentration of each F exposes a hole to a CC on Cr while the valence shell of O exposes a CC to hole on Cr. In the molecules studied in this paper, the CC in the valence shell of an O, C, or H ligand never faces a CC in the metal atom core.

been made by Kang, Tang, and Albright.[20] They found that the trigonal bipyramid is the lowest energy geometry for VF_5 and $TaCl_5$ while the square pyramid is the lowest energy geometry for the hydrides and methanides. These authors rationalized the non-VSEPR geometry of the hydrides on the basis of a small HOMO−LUMO gap that yields a transition density of the symmetry required for a C_{4v} geometry by a second-order Jahn−Teller distortion.[21] Our calculated structures for VF_5, VH_5, and VMe_5 are in good agreement with their work, and with the experimental values[22] for VF_5 of $VF_{ax} = 1.73$ Å and $VF_{eq} = 1.70$ Å.

For VF_5 the trigonal bipyramid geometry has a lower energy than the square pyramid geometry, while for VMe_5 and VH_5 the square pyramid geometry has a lower energy (Table 1). As can be seen from the contour plots of ρ and L in Figure 2 the marked distortion of the core for VMe_5 and VF_5 is evident in ρ and is displayed more clearly in L. These core distortions are shown in another way in the isosurface plots of the vanadium core for VF_5 and VH_5 in Figure 4. It is remarkable that these large *core* distortions can be clearly seen in the electron density contour = 2 au, that is at an electron density that is greater by a factor of approximately 10 than the corresponding distortions in a *valence shell* charge concentration in the main group elements P, S, or Cl. In each case there are five ligand-opposed CC's in the vanadium core, those in VH_5 and VMe_5 being larger than those in VF_5. In the trigonal bipyramidal geometry of each molecule the CC's form a trigonal bipyramid that is rotated 60°

(20) Kang, S. K.; Tang, H.; Albright, T. A. *J. Am. Chem. Soc.* **1993**, *115*, 1971.

(21) Bader, R. F. W. *Mol. Phys.* **1960**, *3*, 137; *Can. J. Chem.* **1962**, *40*, 1164.

(22) Hagen, K.; Gilbert, M. M.; Hedberg, L.; Hedberg, K. *Inorg Chem.* **1982,** *21*, 2690.

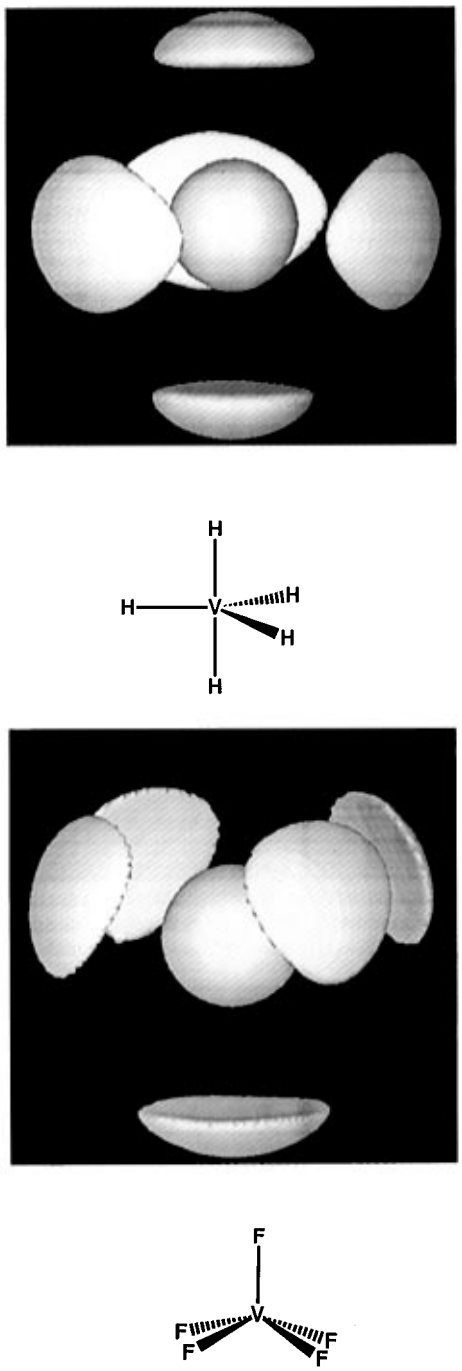

Figure 4. Envelopes of L for $L = 15$ defining the ligand opposed charge concentrations in the outer shell of the core of vanadium in (a, top) VF_5 and (b, bottom) VH_5. In VF_5 the two axial ligands necessarily face CC's while the equatorial ligands and all the ligands in VH_5 face regions of charge depletion in the vanadium core.

around the C_3 axis with respect to the trigonal bipyramid formed by the ligands. In this geometry the two axial ligands face the two axial core CC's while the equatorial ligands are opposite (3, −1) critical points on the edges of the trigonal bipyramid of CC's. In the square pyramid geometry the five CC's form a square pyramid that is inverted with respect to the square pyramid formed by the ligands. In this geometry all the ligands are opposite (3, +1) critical points (regions of maximum charge depletion) in the outer shell of the core and none of them are opposite CC's. The H atom in the hydride and the C atom of the Me ligand have large bonding CC's that avoid the core CC's of the metal and occupy sites opposite the (3, +1) critical points in the faces of the polyhedron of CC's giving a square pyramid geometry, while the less strongly interacting F ligands retain the VSEPR predicted geometry even though each axial ligand faces a CC in the core. Tantalum has a more easily distorted (polarized) core than vanadium, so TaH_5 and $TaMe_5$ are also expected to have a square pyramid geometry as has been found experimentally for $TaMe_5$.[8]

Chromium Hexafluoride and Hexamethanide. Kang, Tang, and Albright[20] have made an extensive study of the calculated structures of $CrMe_6$ at various levels of theory and have shown that the lowest energy geometry is the trigonal prism. They accounted for this structure in terms of a small HOMO−LUMO gap that yields a transition density of the symmetry required for a D_{3h} geometry by a second-order Jahn−Teller distortion.[21] Neuhaus *et al.*[23] have published an extensive study of the effects of changing the basis set and of various post-Hartree−Fock methods on the relative energies of the octahedral and trigonal prism geometries of CrF_6, and they have concluded that the octahedral geometry is the most stable. The results of our calculations (Table 1) are in good agreement with this previous work. Figure 5 shows contour plots of L for the octahedral CrF_6 and for trigonal prismatic $CrMe_6$. We see that the C atom of the methyl group in $CrMe_6$ has a large bonding CC that is not present in the fluoride. Table 3 shows that the core CC's are larger in $CrMe_6$ than in CrF_6 just as we found for VMe_5 and VF_5. In the octahedral geometry of CrF_6 there are six CC's in the core of the chromium atom that have an octahedral arrangement so that each ligand faces one of these CC's. The F ligands, which do not exhibit a bonding CC, do not interact sufficiently strongly with the core to distort the VSEPR geometry that is determined by the interactions between the ligands. In octahedral $CrMe_6$ each carbon atom necessarily faces a CC, but in the lower energy trigonal prism geometry there are only five CC's which have a trigonal bipyramid arrangement with a (3, +1) critical point or region of charge depletion in the center of each of the six faces of the trigonal bipyramid. The (3, +1) critical points therefore have a trigonal prism arrangement, and each of the six methyl ligands has a bonding CC facing each of these six faces so that the Me ligands also have a trigonal prism geometry. Although this geometry increases the interaction between the ligands compared to the octahedral geometry, it decreases the interaction between the ligands and the core and so becomes the stable geometry when the interaction between the ligands and the core is strong enough as in $CrMe_6$. As for VF_5 and VMe_5 the geometry in which the ligands are all facing regions of charge depletion in the core is the favored geometry for the more covalently bound Me ligand, while the more ionically bound CrF_6 retains the VSEPR-predicted octahedral structure. Chromium hexamethyl is the first example that we have discussed in which the core CC's are not ligand opposed. They do however have an arrangement that keeps them as far apart as possible and that is consistent with their arising from the repulsion of the core electrons by the ligands. There is no geometry of six ligands that will give an arrangement of six ligand-opposed CC's such that the ligands all occupy sites opposite the (3, +1) critical points in the faces of the core charge polyhedron. Indeed, if the CC's produced by the ligands in the trigonal prism geometry were ligand opposed they would also have a trigonal prism arrangement such that the ligands would be opposite the (3, −1) critical points in the edges of the CC trigonal prism rather than opposite the (3, +1) critical points in the faces.

Chromium and Molybdenum Oxotetrafluorides. $CrOF_4$ and $MoOF_4$ both have the non-VSEPR square pyramid geometry[9] with oxygen in the axial position (Table 1) in contrast to analogous main group element molecules such as SOF_4 which have the VSEPR predicted trigonal pyramid structure with

(23) Neuhaus, A; Frenking, G.; Huber, H.; Gauss, J. *Inorg. Chem.* **1992**, *31*, 5355.

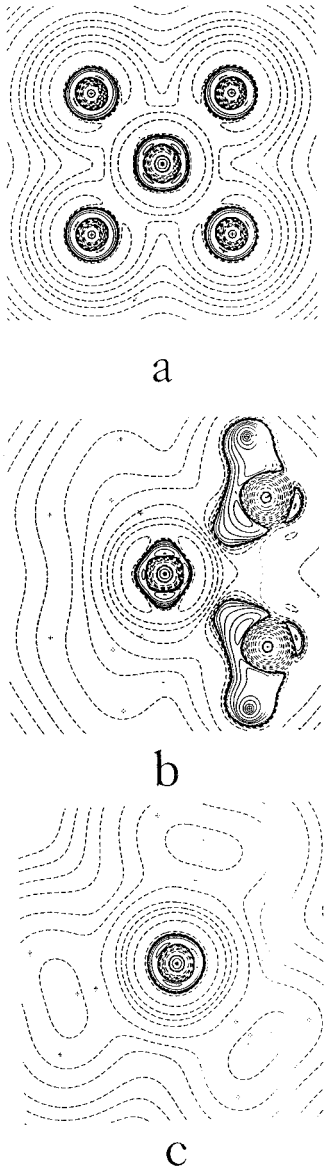

Figure 5. Contour maps of L for octahedral CrF_6 (a) and trigonal prismatic $CrMe_6$ (b and c). The plane in b contains the Cr nucleus and a C−H bond of each of two methyl groups and shows the two axial CC's of the trigonal bipyramidal arrangement of CC's. The plane in c is the σ_h symmetry plane bisecting the molecule and shows the three equatorial CC's.

oxygen in an equatorial position.[1] In agreement with the experimental observations our calculations show that the square pyramid geometry has a lower energy than the trigonal bipyramid geometry for both $CrOF_4$ and $MoOF_4$. Figure 2 shows a contour plot of L for the lower energy square pyramid geometry of $CrOF_4$. As we see in Table 3 the strongly bonded oxygen atom, which has a large bonding CC in its valence shell, produces a correspondingly larger opposing core charge concentration than the more weakly bound F atom which does not exhibit any bonding CC in either molecule. It appears that the doubly bonded oxygen atom distorts the core sufficiently to stabilize the non-VSEPR square pyramid geometry over the trigonal bipyramidal geometry. In particular, in the trigonal bipyramidal geometry the large CC opposed to oxygen makes angles of only 56° with the two closest adjacent fluorine ligands in the equatorial plane, whereas in the square pyramid geometry the oxygen-opposed CC makes larger angles of 75° with each of the four adjacent fluorine ligands, which again favors the square pyramid geometry over the trigonal bipyramid. Even for a molecule such as PF_5 in which the P core is spherical, the square pyramid structure is only of slightly higher energy than the trigonal bipyramid structure so that it does not take a very large distortion of the core to make the square pyramid the lower energy geometry. The difference in geometry between $CrOF_4$ and SOF_4 is somewhat analogous to that between trigonal bipyramidal PF_5, an AX_5 molecule, and square pyramidal ClF_5, an AX_5E molecule, in which the base of the square pyramid (the sixth octahedral position) is occupied by a lone pair, while in $CrOF_4$ it is occupied by the large CC opposite oxygen.

Other related molecules with similar square pyramidal structures include OWF_4, $OWCl_4$, $SWCl_4$, and $SeWCl_4$.[3,24] In a recent paper Neuhaus et al.[18] showed that the calculated structure of $MoNF_4^-$ is square pyramidal. In a study of the Laplacian of the electron density of this and related molecules, they found that the triply bonded nitrogen produces a larger ligand opposed CC than that produced by the singly bonded fluorines, although they did not comment on this. This large CC appears to be responsible for the square pyramidal structure of this ion just as the CC produced by the multiply bonded oxygen is responsible for the square pyramidal geometry of $CrOF_4$ and $MoOF_4$.

Chromium Dioxodifluoride. CrO_2F_2 has the VSEPR predicted tetrahedral geometry, but the FCrF bond angle is slightly larger than the OCrO bond angle (Table 1) and the difference between the experimental angles (O−Cr−O = 107.8° and F−Cr−F = 111.9°)[10] is somewhat greater. These angles are inconsistent with the VSEPR concept that a multiple bond domain (the CrO bond domain) is larger and takes up more space in the valence shell of the central atom than single bond domains (the CrF bond domain) as is the case in the analogous main group molecule SO_2F_2 in which the OSO angle is considerably larger (124°) than the FSF angle (96°).[3,11]

The unexpected bond angles in this molecule are, however, readily understood in terms of the Laplacian of the electron density of the chromium core. The contour and isosurface plots of L in Figure 6 show that there are four ligand opposed CC's in the chromium core that form an approximate tetrahedron that is oriented so that each ligand is opposite a (3, +1) critical point or region of maximum charge depletion in the outer shell of the core, an arrangement that further stabilizes the tetrahedral arrangement of the ligands. However, because the CC's opposed to the oxygen ligands are larger than those opposed to the fluorine ligands, they do affect the bond angles. Both of the OFF faces of the tetrahedron formed by the ligands are enlarged by the interaction of the large oxygen-opposed CC's with these ligands thereby increasing the FCrF bond angle and decreasing the OCrO bond angle so that the OCrO angle is smaller, rather than larger than, the FCrF angle (Figure 6).

Similar results have been obtained by MacDougall and Hall for CrO_2Cl_2[25] and have been explained by them in a similar way. In a similar study of $VOCl_3$ a large core CC opposed to oxygen was observed.[26] As this CC is located between the Cl ligands it increases the ClVCl angles so that they are larger than the tetrahedral angle instead of smaller as predicted by the VSEPR model.

The Oxopentafluorochromium Anion, $CrOF_5^-$. The approximately octahedral structure of this ion[23] conforms to the predictions of the VSEPR model in that the four fluorine atoms in a plane are bent away from the oxygen, consistent with the CrO bond having some multiple bond character and the oxygen being less electronegative than fluorine. There are five ligand-opposed charge concentrations, one opposite four of the fluorine ligands and a larger one opposite oxygen, with an overall square

(24) Cotton, A. Wilkinson, G. *Advanced Inorganic Chemistry*, 5th ed.; Wiley Interscience: New York, 1988.
(25) MacDougall, P. J.; Hall, M. B. *Trans. Am. Crystallogr. Assoc.* **1990**, *26*, 101.

Table 3. Properties of Metal Atom Core Charge Concentrations

	CC's					
molecule	geometry	opposed atom	number	∠CC−M−CC (deg)	*L* (au)	*r*(M)[a] (au)
VF5(tbp)	tbp	F_{ax}	2	90.0	17.1	0.720
		F_{eq}	3	120.0	18.8	0.716
VF_5(sp)	sp	F_{ax}	1	106.4 (ax−M−ba)	19.7	0.714
		F_{ba}	4	85.4 (ba−M−ba)	17.5	0.719
VH_5(tbp)	tbp	H_{ax}	2	90.0	24.1	0.708
		H_{eq}	3	120.0	22.6	0.710
VH_5(sp)	sp	H_{ax}	1	114.1 (ax−M−ba)	16.2	0.722
		H_{ba}	4	80.4 (ba−M−ba)	20.5	0.715
VMe_5(sp)	sp	C_{ax}	1	102.7 (ax−M−ba)	21.0	0.712
		C_{ba}	4	87.3 (ba−M−ba)	23.2	0.170
CrF_6(oct)	oct	F	6	90.0	24.5	0.665
CrF_6(tp)	tp	F	6	93.7,[b] 69.8[c]	23.5	0.667
$CrMe_6$(tp)	tbp		3	120.0	24.4	0.667
			2	90.0	41.1	0.642
$CrOF_4$(tbp)	tbp	F_{ax}	2		22.5	0.669
		F_{eq}	2	96.6 (eq−M−eq)	25.1	0.664
		O_{eq}	1	105.9 (ax−M−eq)	28.8	0.659
$CrOF_4$(sp)	sp	O_{ax}	1	101.5 (ax−M−ba)	28.6	0.660
		F_{ba}	4	87.7 (ba−M−ba)	23.9	0.666
$MoOF_4$(tbp)	tbp	F_{ax}	2	94.5 (ax−M−O)[d]	2.7	1.052
		F_{eq}	2	108.5 (eq−M−eq)	3.2	1.049
		O_{eq}	1		4.2	1.043
$MoOF_4$(sp)	sp	O_{ax}	1	103.6 (ax−M−ba)	4.2	1.045
		F_{ba}	4	86.8 (eq−M−eq)	3.0	1.050
CrO_2F_2(tet)	tet	F	2	122.7 (F−M−F)[d]	24.1	0.665
		O	2	99.6 (O−M−O)[d]	28.4	0.660
$CrOF_5^-$(oct)	sp	F_{eq}	4	88.3 (ba−M−ba)	21.8	0.670
		O	1	100.1 (ax−M−ba)	23.2	0.667
cis$CrO_2F_4^{2-}$(oct)	tet	O	2	100.0 (O−M−O)[d]	24.1	0.666
			2		19.7	0.672
trans$CrO_2F_4^{2-}$	cube		8	70.5	20.4	0.671

[a] Distance of charge concentration from metal atom nucleus. [b] Angle between CC's in opposite triangular faces of the trigonal prism. [c] Angle between CC's in the same triangular face of the trigonal prism. [d] Angle between the CC's opossed to the designated atoms.

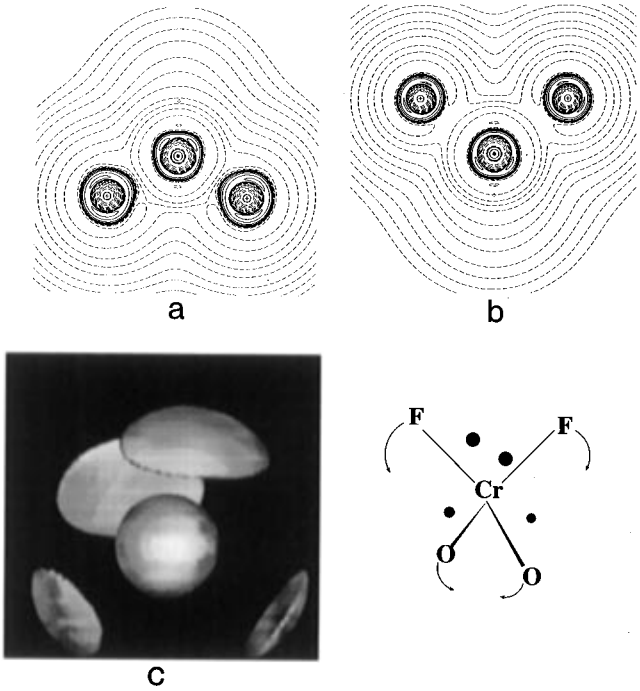

Figure 6. Contour and envelope maps of *L* for CrO2F2. (a) Contour map of the O−Cr−O plane showing the two ligand opposed CC's in the Cr core. (b) Contour map of the F−Cr−F plane showing the other two ligand opposed CC's that form an overall tetrahedral arrangement of CC's. (c) Envelope map illustrating the tetrahedral arrangement of the CC's and the larger size of the CC's opposed to the oxygen atoms.

pyramid arrangement (Figure 7a). Four fluorine ligands and the oxygen ligand are opposite (3, +1) critical points in the Laplacian of the core density while the fifth fluorine is opposite a (3, −3) CC. If each ligand produced a ligand opposed core charge concentration there would be a sixth CC. The one that is missing would be facing the oxygen CC, consistent with our general observation that a strongly interacting ligand such as =O, H, or Me is never located facing a core CC but always faces a region of maximum charge depletion.

The Dioxopentafluorochromium(VI) Anion $CrO_2F_4^{2-}$. The stable isomer of this ion has the *cis* structure.[11] The CrO bonds are rather short, suggesting that they have some double bond character. According to the VSEPR model multiple bond domains tend to keep as far apart as possible thus favoring the *trans* rather than the *cis* structure for $CrO_2F_4^{2-}$. It seems reasonable to suppose that the preference for the *cis* structure is a consequence of a nonspherical core resulting from the distortion produced by the ligands. We see in Figure 7 that in the *cis* isomer there are four charge concentrations, one opposed to each oxygen and two on a plane bisecting the OCrO angle giving an overall tetrahedral arrangement. The O ligands are opposite two of the faces of this tetrahedron, that is (3, +1) critical points. The two axial fluorines are opposite the other two faces of the tetrahedron and the other two are opposite two vertices of the tetrahedron. We note that again in this case there are no charge concentrations facing the O ligands which always prefer to face regions of maximum charge depletion. In the less stable *trans* isomer there are eight core CC's with an overall cubic arrangement. The O ligands are opposite two opposing faces of this cube and the fluorines are opposite four of the edges, that is opposite (3, −1) critical points. Although the oxygen ligands are facing (3, +1) critical points in both the *cis* and *trans* isomers they face larger depletions of charge in the faces of the tetrahedron of CC's in the *cis* isomer than in the faces of the cube of CC's in the *trans* isomer. Moreover the

(26) MacDougall, P. J.; Hall, M. B.; Bader, R. F. W.; Cheeseman, J. R. *Can. J. Chem.* **1989**, *67*, 1842.

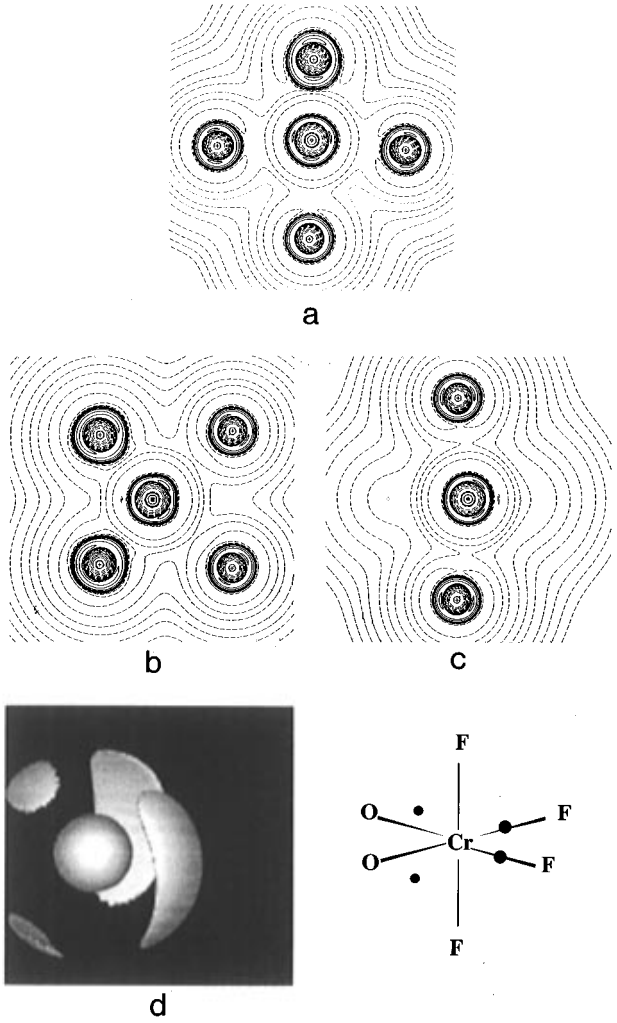

Figure 7. (a) Contour map of L for $CrOF_5^-$ in the plane through the O nucleus and three F nuclei. Note the absence of a CC opposed to the axial F in the outer shell of the core of Cr, one that would face the CC in the valence shell of O. (b) Contour map of L for *cis* $CrO_2F_4^{2-}$ for the plane containing the Cr nucleus, the two O nuclei and two F nuclei. (c) Contour map of L for the plane bisecting the O−Cr−O angle. The plots (b) and (c) contain an extra contour for $L = 18$ to show the CC's in the Cr core. (d) Envelope map for $L = 19$ showing the approximately tetrahedral arrangement of the two large CC's opposed to the O atoms and the two smaller CC's in the plane shown in c.

tetrahedral arrangement of charge concentrations is expected to be a lower energy arrangement that the cube of eight CC's. So the *cis* isomer is the preferred geometry for this molecule.

There are many related complexes of Mo(VI) such as $MoO_2Cl_4^-$, $MoO_2Cl_2(H_2O)_2$, and $MoO_2(OPPh_3)_2$ which also have approximately octahedral structures with *cis* oxygen atoms,[24] presumably for the same reasons as we have discussed.

Summary and Conclusions

The results reported in this paper show the following.

(1) The bonds between the metal atom and the O, CH_3, and H ligands in V(V) and Cr(VI) molecules are predominately covalent while the bonds to fluorine are predominately ionic.

(2) The V(V) and Cr(VI) cores in the molecules studied are distorted, giving the core a nonspherical shape. A similar distortion of the cores of Mo(VI), W(VI), Re(VII), and Os(VI) was observed by Neuhaus *et al.*[18] but was not commented upon by them.

(3) The distortion of the metal core is produced by the interaction of the ligands with the core. In most cases, as a consequence of electrostatic repulsion and the operation of the Pauli principle, each ligand produces a charge concentration on the opposite side of the core (a ligand-opposed charge concentration).

(4) The geometry of a transition metal molecule is determined by three interactions: ligand−ligand, ligand−CC and CC−CC.

When the core-ligand interaction is weak, or the ligand−ligand interaction is strong, the ligand−ligand interaction dominates, as in the more ionically bound fluorides (VF_5 and CrF_6), and the molecule has the geometry which minimizes the ligand−ligand interaction, that is the VSEPR geometry (AX_4, tetrahedral; AX_5, trigonal bipyramid; AX_6, octahedral). When the ligands have this geometry the ligand opposed CC's also necessarily have the same minimum energy geometry. When the interaction between the core and the ligands is strong (and/or the interaction between the ligands is weak) as in the more covalently bound hydrides and methanides (VH_5, VMe_5, and $CrMe_6$) the core−ligand interactions dominate the geometry and neither the CC's nor the ligands necessarily have a minimum energy arrangement. In each case the ligands adopt positions facing regions of maximum charge depletion, that is opposite the faces of the polyhedron formed by the charge concentrations, thereby minimizing the ligand−CC interaction. In VH_5 and VMe_5 the ligands adopt a square pyramidal geometry opposite the five faces of the corresponding square pyramidal arrangement of ligand-opposed CC's. The square pyramidal geometry of the ligands and the corresponding square pyramidal geometry of the CC's are slightly less favorable than the trigonal bipyramidal arrangement but the ligand−CC interaction is minimized, so that this is the minimum energy geometry. In $CrMe_6$ the ligands adopt a trigonal prism geometry opposite the six faces of a trigonal bipyramid arrangement of five charge concentrations that are, in this case, not ligand opposed, but this geometry minimizes their mutual interaction. This arrangement of ligands is slightly less favorable than the octahedral arrangement but it minimizes the ligand−CC interactions, so that the trigonal prism is the minimum energy geometry.

In $CrOF_4$ and $MoOF_4$ the strongly bonded oxygen interacts sufficiently strongly with the core to make the square pyramid geometry favored over the trigonal bipyramidal geometry observed for VF_5. In CrO_2F_2 the tetrahedral minimum energy geometry of the ligands also produces a tetrahedral minimum energy arrangement of ligand-opposed CC's so that the overall geometry is approximately tetrahedral. But it is distorted from that observed in the analogous main group molecule SO_2F_2 by the stronger interaction of the oxygen ligands than the fluorine ligands with the core.

Before we are in a position to confidently predict the geometry of metal molecules it will be necessary to study the core distortion in a wider selection of molecules, including metals with d^1−d^{10} configurations. In a first step in this direction we have recently shown that the d^{10} core of zinc in $ZnCl_4^{2-}$ is tightly held and spherical in shape so that this ion has a tetrahedral geometry. Until we have this additional information, however, it is of interest to make some provisional predictions for d^0 metal molecules just on the basis that core CC's adopt the arrangement that minimizes (or nearly minimizes) their mutual interaction; the tetrahedral arrangement for four CC's, the trigonal bipyramidal or the slightly higher energy square pyramidal arrangement for five CC's and the octahedral arrangement for six CC's. In Table 4 we denote a ligand, such as =O or CH_3, that interacts strongly with the core by L and a ligand, such as F, that interacts weakly with the core by X.

The tetrahedral arrangement of four CC's has four regions of maximum charge depletion (3, +1) critical points, one in each face of the tetrahedron of CC's, so that we predict that ML_2 molecules will have an angular shape, ML_3 molecules a pyramidal shape, and ML_4 molecules a tetrahedral shape. MX_2,

Table 4. Predicted Geometries for d^0 Molecules with Weak Ligands X and Strong Ligands L

group	2	13	14	15	16
example	CaX_2	ScX_3	TiX_4	VX_5	CrX_6
VSEPR geometry	linear	triangular	tetrahedral	trigonal bipyramidal	octahedral
example	CaL_2	ScL_3	TiL_4	VL_5	CrL_6
number of CC's	4	4	4	5	5
geometry of CC's	tetrahedral	tetrahedral	tetrahedral	square pyramidal	trigonal bipyramidal
geometry of molecule	angular	pyramidal	tetrahedral	square pyramidal	trigonal prismatic

MX_3, and MX_4 molecules, in which ligand−ligand repulsions dominate, will have the VSEPR predicted geometries, namely MX_2 linear, MX_3, planar triangular, and MX_4 tetrahedral. We note that the tetrahedral geometry of a four-coordinated metal molecule is independent of the strength of the interaction of the ligands with the core. All known AX_4 and AL_4 metal molecules have a tetrahedral geometry. Although there appear to have been no experimental studies of d^0 transition metal AX_3 or AL_3 molecules it is interesting to note that the molecules, ScH_3, TiH_3^+, and $TiMe_3^+$ have been computed to have the pyramidal geometry predicted for AL_3 molecules.[27,28]

The square pyramid arrangement of five CC's has five (3, +1) critical points (regions of maximum charge depletion) to accommodate five ligands in a low energy square pyramidal geometry. In contrast the trigonal bipyramidal arrangement of five CC's has six (3, + 1) critical points, one in the center of each of its six faces, with a trigonal prism arrangement. Placing five ligands opposite five of these faces gives a much less favorable arrangement of the ligands than the square pyramid arrangement. Thus ML_5 molecules are predicted to have a square pyramidal geometry based on a square pyramidal arrangement of CC's. In MX_5 molecules ligand−ligand interactions dominate, giving the trigonal bipyramidal geometry.

If each of the six faces of the trigonal bipyramidal arrangement of five CC's are occupied by strongly interacting ligands, we get an ML_6 molecule with a trigonal prism geometry as has been observed for WMe_6 and calculated for $CrMe_6$. This geometry has also been observed for the the solid state structure of MoS and it seems reasonable to suppose that in this case also where Mo has a d^2 configuration the Mo core has five CC's with a trigonal bipyramidal arrangement. The octahedral arrangement of six charge concentrations has eight (3, +1) critical points in a cubic arrangement. Occupation of six of these sites by bonding domains would give a geometry with a much higher energy than the octahedron or the trigonal prism so the octahedral geometry is found only for MX_6 molecules whereas ML_6 molecules adopt the trigonal prism geometry as we have seen.

Finally it should be noted that the electron localization function ELF, introduced by Becke and Edgecombe,[29] has recently been shown[30] to provide a description of electron localization equivalent to that provided by the CC's of the Laplacian. In particular, both ELF and the Laplacian predict the same pattern of ligand-opposed electron domains in the outer shell of the core of the transition metal atoms in the molecules discussed in this paper.

Acknowledgment. We thank the Natural Science and Engineering Research Council of Canada for financial support, and we thank Robert deWitte for carrying out some of the calculations on $CrOF_4$ and $MoOF_4$.

IC9514206

(27) Jolly, C. A.; Marynick, D. S. *Inorg. Chem.* **1989**, *28*, 2893.
(28) Musaev, D. G.; Charkin, O. P. *Koord. Khim.* **1989,** *5*, 1457.
(29) Becke, E. D.; Edgecombe, K. E. *J. Chem. Phys.* **1990**, *92,* 5397.
(30) Bader, R. F. W.; Johnson, S.; Tang, T.-H.; Poppelier, P. L. *J. Phys. Chem.*, submitted for publication.